IFMBE Proceedings 114

Fernando Emilio Ballina
Ricardo Armentano
Rubén Carlos Acevedo
Gustavo Javier Meschino *Editors*

# Advances in Bioengineering and Clinical Engineering

## Proceedings of the XXIV Argentinian Congress of Bioengineering (SABI 2023), October 3–6, 2023, Buenos Aires, Argentina - Volume 2

Springer

# IFMBE Proceedings 114

The IFMBE Proceedings Book Series is an official publication of *the International Federation for Medical and Biological Engineering* (IFMBE). The series gathers the proceedings of various international conferences, which are either organized or endorsed by the Federation. Books published in this series report on cutting-edge findings and provide an informative survey on the most challenging topics and advances in the fields of medicine, biology, clinical engineering, and biophysics.

The series aims at disseminating high quality scientific information, encouraging both basic and applied research, and promoting world-wide collaboration between researchers and practitioners in the field of Medical and Biological Engineering.

Topics include, but are not limited to:

- Diagnostic Imaging, Image Processing, Biomedical Signal Processing
- Modeling and Simulation, Biomechanics
- Biomaterials, Cellular and Tissue Engineering
- Information and Communication in Medicine, Telemedicine and e-Health
- Instrumentation and Clinical Engineering
- Surgery, Minimal Invasive Interventions, Endoscopy and Image Guided Therapy
- Audiology, Ophthalmology, Emergency and Dental Medicine Applications
- Radiology, Radiation Oncology and Biological Effects of Radiation
- Drug Delivery and Pharmaceutical Engineering
- Neuroengineering, and Artificial Intelligence in Healthcare

IFMBE proceedings are indexed by SCOPUS, EI Compendex, Japanese Science and Technology Agency (JST), SCImago. They are also submitted for consideration by WoS.

Proposals can be submitted by contacting the Springer responsible editor shown on the series webpage (see "Contacts"), or by getting in touch with the series editor Ratko Magjarevic.

Fernando Emilio Ballina · Ricardo Armentano ·
Rubén Carlos Acevedo ·
Gustavo Javier Meschino
Editors

# Advances in Bioengineering and Clinical Engineering

## Proceedings of the XXIV Argentinian Congress of Bioengineering (SABI 2023), October 3–6, 2023, Buenos Aires, Argentina - Volume 2

Springer

*Editors*
Fernando Emilio Ballina
Instituto de Ingeniería y Agronomía
National University Arturo Jauretche
Florencio Varela, Buenos Aires, Argentina

Rubén Carlos Acevedo
Facultad de Ingeniería
Universidad Nacional de Entre Ríos
Oro Verde, Argentina

Ricardo Armentano
EMBS IEEE Technical Committee on
Cardiopulmonary Systems
and Physiology-Based Engineering
New Jersey, USA

Gustavo Javier Meschino
Instituto de Investigaciones Científicas y
Tecnológicas en Electrónica
Universidad Nacional de Mar del Plata
Mar del Plata, Argentina

ISSN 1680-0737 ISSN 1433-9277 (electronic)
IFMBE Proceedings
ISBN 978-3-031-61972-4 ISBN 978-3-031-61973-1 (eBook)
https://doi.org/10.1007/978-3-031-61973-1



This Springer imprint is published by the registered company Springer Nature Switzerland AG
The registered company address is: Gewerbestrasse 11, 6330 Cham, Switzerland

# Preface

The XXIV Bioengineering Congress and XIII Clinical Engineering Conference (SABI 2023) was held in the Ciudad Autónoma de Buenos Aires (Argentine) and in the city of Florencio Varela from October 3–6, 2023. The event represents the scientific meeting of the Argentine Society of Bioengineering, and on this occasion, it was organized by the Arturo Jauretche University.

The congress covered topics such as bioinstrumentation, digital signal processing and biomedical images, rehabilitation engineering, biomaterials and tissue engineering, clinical engineering, bioinformatics, modeling and simulation of biological systems, medical informatics, education, among others.

The IFMBE organized a special session on Biomedical Engineering Education for professionals and students as well as a special session on Women in Biomedical Engineering.

As a satellite event of the congress, the so-called Student SABI was held, an event aimed especially at students in which presentations by specialists, 37 works showcased, workshops, and visits to companies were held. The objective of this event is to strengthen the bond between students from different universities and promote the exchange of experiences between them.

It is both our pleasure and honor to extend a cordial welcome to all participants actively engaging in the exploration of the proceedings of SABI 2023. The conference showcased an impressive array of over 145 research papers and ten conferences by international experts, all converging to deliberate on the challenges intrinsic to the advancement of future technologies in medicine and biology.

Conferences of this nature inherently serve the purpose of facilitating social interactions among individuals who share common interests and expertise. These gatherings provide attendees with the opportunity to extract novel insights, exchange prevailing ideas, and delve into critical aspects of healthcare. This conference, therefore, stands as an invaluable platform not only to stay updated within one's specific area of expertise but also to explore the forefront of advancements in other domains. While an attendee's specialization may extend beyond the realm of Medical and Biological Engineering, the compilation of works presented herein holds the potential to provide noteworthy insights capable of revolutionizing approaches to broader challenges.

We are confident that each of you found considerable satisfaction in the extensive opportunities offered during SABI 2023. The event proved to be a remarkable confluence of experiences and expertise spanning a wide spectrum of fields, all encapsulated under a unified roof. This collaborative endeavor has undoubtedly sparked a tangible wave of motivation and diversity, resonating not only across the Americas but also reverberating throughout the global landscape.

# Organization

## Committees

### Conference Chair

| | |
|---|---|
| Fernando Ballina | Instituto de Ingeniería y Agronomía, Universidad Nacional Arturo Jauretche, Buenos Aires, Argentina |

### Scientific Chair

| | |
|---|---|
| Ricardo Armentano | EMBS IEEE Technical Committee on Cardiopulmonary Systems and Physiology-Based Engineering, New Jersey, USA |

### Scientific Committee Members

| | |
|---|---|
| Ruben Acevedo | Universidad Nacional de Entre Ríos |
| Enrique Avila Perona | Universidad Nacional de San Juan |
| Fernando Ballina | Universidad Nacional Arturo Jauretche |
| Ramiro Barreiro Saravia | Ministerio de Salud Pública de Salta |
| Maria Belluzo | Universidad Nacional de La Plata |
| Diego Beltramone | Universidad Nacional de Córdoba |
| Martin Belzunce | Universidad Nacional de San Martín |
| Paula Bonomini | Instituto Tecnológico de Buenos Aires |
| Ariel Braidot | Universidad Nacional de Entre Ríos |
| Diego Campana | Universidad Nacional de Entre Ríos |
| Victor Carmona | Universidad Nacional de San Juan |
| Carolina Carrere | Universidad Nacional de Entre Ríos |
| Mariano Casciaro | Universidad Favaloro |
| Paola Catalfamo Formento | Universidad Nacional de Entre Ríos |
| Santiago Collavini | Universidad Nacional Arturo Jauretche |
| Diego Comas | Universidad Nacional de Mar del Plata |
| Damian Craiem | Universidad Favaloro |
| Ronald Del Aguila Heidenreich | Universidad Nacional de Córdoba |
| Juan Fernández | Universidad Nacional de La Plata |
| Mariano Fernandez Corazza | Universidad Nacional de La Plata |

| | |
|---|---|
| Lucila Figueroa Gallo | Universidad Nacional de Tucumán |
| Jose Gallardo | Instituto Universitario del Hospital Italiano |
| Pablo Gleiser | Instituto Tecnológico de Buenos Aires |
| Sebastian Graf | Universidad Favaloro |
| Juan Graffigna | Universidad Nacional de San Juan |
| Alejandro Hadad | Universidad Nacional de Entre Ríos |
| Ramiro Irastorza | Universidad Nacional Arturo Jauretche |
| Sergio Liberczuk | Universidad Nacional Arturo Jauretche |
| Rossana Madrid | Universidad Nacional de Tucumán |
| Ana Carolina Maldonado | Universidad Nacional de Córdoba |
| Maria Carla Mantaras | Universidad Nacional de Entre Ríos |
| Ignacio Marolla | Universidad Nacional Arturo Jauretche |
| Ezequie Mazzoni | Universidad Nacional Arturo Jauretche |
| Gustavo Meschino | Universidad Nacional de Mar del Plata |
| Carlos Muravchik | Universidad Nacional de La Plata |
| Tamara Oberti | Universidad Nacional de La Plata |
| Juan Manuel Olivera | Universidad Nacional de Tucuman |
| Federico Paschetta | Instituto Tecnológico de Buenos Aires |
| María Perez | Universidad Nacional de San Juan |
| Pablo Peruzzo | Universidad Nacional de La Plata |
| Sergio Ponce | Universidad Tecnológica Nacional |
| Agustina Portu | Universidad Nacional de San Martín |
| Emiliano Ravera | Universidad Nacional de Entre Ríos |
| Marcelo Risk | Instituto Universitario del Hospital Italiano |
| Héctor Rodrigo | Universidad Nacional de San Juan |
| Jorge Daniel Romero | Ministerio de Salud de Tierra del Fuego |
| Débora Rubio | Universidad Tecnológica Nacional |
| Eduardo SALINAS | Universidad Nacional Arturo Jauretche |
| Enrique Spinelli | Universidad Nacional de La Plata |
| Carolina Tabernig | Universidad Nacional de Entre Ríos |
| Emanuel Tello | Universidad Nacional de San Juan |
| Rosa Weisz | Universidad Nacional de Entre Ríos |
| Sandra Wray | Instituto Universitario del Hospital Italiano |
| Bonifacio Zanutto | Universidad de Buenos Aires |

# Contents

**Biomedical Signal Processing**

Improved ERD Detection of EEG Sensorimotor Rhythms Through Wavelet Transform . . . . . . . . . . 3
*Alejandro Quiroga, Diana Vértiz del Valle, Katherine Tschopp, Leonardo Rufiner, and Rubén Acevedo*

Optimized Transcranial Brain Stimulation for Tumor Treating Fields . . . . . . . . . . 14
*Dante C. Andrinolo O., Mariano Fernández-Corazza, and Carlos H. Muravchik*

High Frequency Oscillation in Epilepsy: Review . . . . . . . . . . 22
*Rocio Buenamaizon, Juan Pablo Graffigna, Otoya Raúl, and Fernando Icazatti*

Non-invasive Recording of Physiological Variables Under Stress Conditions and Aerobic and Anaerobic Physical Activity . . . . . . . . . . 30
*Andrea Hongn, Facundo Bosch, L. E. Prado, J. M. Ferrández, and M. Paula Bonomini*

Characterisation of EEG Activity in Stimulation and Rest Periods by Analysis of Steady-State Visual Evoked Potentials . . . . . . . . . . 40
*Gerardo L. Padilla, Leonardo A. Cano, Facundo A. Lucianna, Eduardo O. Freire, Celia E. Tagashira, and Lucas P. Acosta*

Predictive Diagnosis of Hypertrophic Cardiomyopathy Using Novel Dynamic Vectorcardiogram Markers . . . . . . . . . . 49
*Marina del Milagro Gómez, Pedro David Arini, Guillermo J. Ortega, Dafne Villani, Alberto Cecconi, Jesús Jimenez Borreguero, and Pablo Daniel Cruces*

Algorithm and Validation Method for Spike Sorting Based on Wavelet Analysis and a Genetic Algorithm . . . . . . . . . . 57
*Federico Alscher, Rocío A. Lenzi, Pamela Pérez Escobar, Sebastián O. Villafañe, and Daniela S. Andres*

Segmentation of the Human Gait Cycle Using Hidden Markov Models (HMM) . . . . . . . . . . 68
*Diego Edwards Molina, Mónica T. Miralles, and Raúl Florentin*

A Model of Mechanical Dyssynchrony Based on ECG Features .............. 88
*Beatriz C. Macas, J. M. Ferrández, D. V. Orellana, M. A. Suing, and M. Paula Bonomini*

Preliminary Study of the Application of Dynamic Speckle Pattern Analysis for Toxicants Detection Based on Bacterial Motility Changes ................ 95
*Marcelo Nicolás Guzmán, Melina Nisenbaum, Estefany Cujano Ayala, Silvia Murialdo, and Gustavo Javier Meschino*

Surface EMG Recordings in Freely Moving Rats: A Promising Method for Motor Evaluation and for Minimizing Animal Use in Research ............ 102
*Luciano Rivolta, Leonardo A. Cano, Celia Tagashira, Rodrigo Marañon, Fernando Farfan, and Ana Lía Albarracín*

Preliminary Study on the Identification of Electromyographic Patterns Associated with Musical Performance Movements ......................... 111
*Celia E. Tagashira, Leonardo A. Cano, Luciano Rivolta, Gonzalo D. Gerez, María S. García, and Ana L. Albarracin*

**Biomodels and 3D Printing**

Design and Assembly of a 3D Bioprinter and Characterization of 3D Scaffolds Produced by Casting or Printing ............................... 125
*Daniela A. C. Belmonte, Victoria B. Molina, Joaquín H. Palma, Marcos Bertuola, and Élida B. Hermida*

Porosity Analysis in 3D Printed Scaffolds of Collagen and Hyaluronic Acid Using Image Processing of Scanning Electron Microscopy .............. 135
*Pablo A. Fernández, Romina Comín, Nancy Salvatierra, Juan Pablo Real, and Mariana Cid*

Development of a Low Budget 3D Printed Otolaryngology Simulator: The New Advance in Medical Education .................................... 143
*Anna Bianca Marzetti Biggi, Maria Albertina Loureyro, Federico Agustin Paternostro, Lautaro Ignacio Acosta, Vitas Ciabis, and Santiago Ricard Kin*

Tensile Test on PETG Test Tubes as Material Validation for Application in UL Rehabilitation Prototypes .................................... 149
*Emilio R. Kenan, Marcela V. Céspedes, and Natalia M. López*

Design and Development of a 3D Printed Electrode Headset for Affordable and Reliable Electroencephalography .................................. 159
*Lorenzo A. Bernardi, Octavio G. Haeublein, and Daniel. Zapata*

## Clinical Engineering

Design and Development of a Computerized Maintenance Management System for Medical Equipment . . . . . 171
*Alejandro Vitale and Sergio Antúnez*

FollowING: A Cardiovascular Healthcare Oriented Device . . . . . 179
*Gisela Farace, Hernan Rodriguez, Martín De Luca, Maximiliano Castro Miranda, Tobías Bavasso Piizzi, Facundo Ruderman, Sergio Villegas, Ricardo L. Armentano, and Leandro Javier Cymberknop*

Quality Guidelines in Clinical Engineering Units of Argentina . . . . . 188
*Jorge Daniel Romero and Enrique M. Avila Perona*

Analysis of Human Resources Management and Structures in Clinical Engineering Units of Argentina . . . . . 198
*Jorge Daniel Romero and Enrique M. Avila Perona*

Analysis and Survey of Domestic Sphygmomanometers . . . . . 216
*Paez Cintia, Morales Valentina, Treo Ana Luz, Pulenta Luis, Buenamaizón Rocío, Quiroga Gonzalo, Sánchez Mariana, Valdez Andrés, Ibazeta Ailín, and Gómez Mauricio*

Design and Development of Analyzer Equipment Prototype of Physical Parameters in Neonatal Incubators . . . . . 227
*Amilcar Manuel Bonino, Diego Miguel Rodríguez, and Ronald Del Águila Heidenreich*

Mammograph Territorial Distribution and Replacement Planning in Uruguay . . . . . 250
*Oscar F. Cossio-Ortega, Isabel Morales, Fabiola M. Martinez-Licona, and Franco Simini*

Management and Evaluation of Biomedical Equipment and Installations at CAMEC, Outpatient Clinics and Tertiary Hospital of Uruguay . . . . . 262
*Carlette Duarte, Sergio Camacho, Gastón Nicoloff, Isabel Morales, and Franco Simini*

Safety Layer Design for Improved Glucose Regulation in Artificial Pancreas Systems . . . . . 272
*Fernando Leonel Da Rosa Jurao, Melina Montero, Emilia Fushimi, Nicolas Rosales, and Fabricio Garelli*

Analysis of Mammography Machine Needs in Mexico and Uruguay .......... 286
*Oscar F. Cossio-Ortega, Franco Simini, and Fabiola M. Martinez-Licona*

Wearable Medical Devices: Regulatory Affairs in Argentina .................. 297
*Theo Rodriguez Campos and Leandro N. Monsalve*

Unveiling Medical Oxygen Utilization Through Survey Insights: A Study of Practices in Argentina ........................................................ 306
*R. L. Gutiérrez Candia, Claudia E. Bonell, L. D. Larrateguy, and D. O. Kadur El Ainie*

Internship, Residency, Audit and Service Partnership in Clinical Engineering .............................................................. 317
*Franco Simini and Isabel Morales*

Risk Management Program Applied to the Use of Biomedical Technology ..... 325
*Débora Rubio, María Guadalupe Salguero, Matías Castañeira, Sergio Ponce, and Francisco Madrid*

**Education**

Development of an Orthosis for Radial Nerve Palsy: A Project-Based Learning Experience ....................................................... 341
*Mariana B. Rios, Natalia P. Perdiz, Candela B. Fernandez, Kaylee D. Haggerty, Josefina Ortiz, Paz L. Salvador, Moira Z. Cívico Sintra, Ángel F. Ávila Ventre, Valeria B. Cenicero, María M. Pozo, Paula Simaro, Marcelo R. Risk, and José M. Gallardo*

Degree Integration Projects in Biomedical Engineering: Design of a Didactic Sequence to Promote Learning ................................ 350
*Lucila M. Figueroa Gallo, María F. Lencina, Facundo A. Lucianna, Carmelo Felice, and Rossana Madrid*

An Experience on Application of Learning Based on Project for Teaching Modelling in Physiology ................................................ 359
*María I. Pisarello, Christian M. Torres Salinas, Eduardo L. Marquez Burgos, and Raúl G. Gómez Cedrón*

**Medical Informatics**

RCP Ya! A Mobile Application for Assisting People Suffering from Cardiovascular Events ............................................... 371
*Nicolás Coen, Tomás Antonio, Laura Lazzatti, Melanie Escobar, Ricardo L. Armentano, and Leandro J. Cymberknop*

Medical Informatics and Electrical Safety for Health Sciences Curricula: Fifteen Years of Teaching ........ 380
*Carolina Arámbulo, Natalia Garay, and Franco Simini*

**Medical Physics**

Automated PET Quantification of [$^{18}$F]FDG PET Images for Neurodegenerative Disorders Research ........ 395
*Sol A. Cataldo, Florencia Sarmiento Laspiur, and Martín A. Belzunce*

Measurements of Density and Attenuation Coefficients for Compressible Samples Simulating Breast Tissue ........ 404
*Rosana Pirchio and Ezequiel Adrian Minniti*

Case Study of Solar Risk for a Fisherman in Fray Bentos, Uruguay ........ 414
*Felipe Gorla Gargano, Jorge O. Noir, and Graciela M. Salum*

**Modeling and Simulation of Biomedical Systems**

Computer Modeling of Radiofrequency Thermocoagulation (RF-TC) Using the Recording Intracerebral Electrodes Implanted for Stereo Electroencephalography (SEEG) Monitoring ........ 425
*Santiago Collavini, Juan J. Pérez, Enrique Berjano, Mariano Fernández-Corazza, Silvia Oddo, and Ramiro Irastorza*

Enhanced Empirical Modeling of Electrophysiological Activity in a Bundle of Myelinated Nerve Fibers: An Open-Source Implementation ........ 432
*Facundo A. Lucianna, Rosa M. Serra, Carla B. Goy, Cecilia Saavedra Fresia, Silvina Real, Gerardo L. Padilla, Ana L. Albarracín, and Fernando D. Farfán*

Decoding Motor Decision-Making Patterns: An EEG and EMG Connectivity Modeling Approach ........ 444
*Leonardo Ariel Cano, Gerardo Luis Padilla, Alvaro G. Pizá, Lucas Pedro Acosta, Gonzalo Daniel Gerez, and María S. García*

CInsertion - A Virtual Surgical Simulator for Training the Insertion of Intracochlear Electrodes ........ 454
*Clara Martinez Sarrasague, Natasha Itzcovich, and Ricardo Luis Marengo*

Age Dependence of Central Pressure Generalized Transfer Function: An in Silico Approach . . . . . . . . . . 469
*Ignacio Abal, Rodrigo Canaglia, Eugenia Ipar, Ricardo L. Armentano, and Leandro J. Cymberknop*

Epileptogenicity and Connectivity Analysis in Epilepsy Surgery . . . . . . . . . . 476
*Rocio Buenamaizon, Juan Pablo Graffigna, Rodolfo Rodríguez Schmädke, Otoya Raúl, Graciana Galiana, Jorge Rasmussen, and Omar Urquizu*

**Neuromuscular Systems and Rehabilitation Engineering**

*IM-tention*: A Software for Brain-Computer Interface with Motor Recovery Purposes . . . . . . . . . . 489
*Vertiz del Valle Diana, L. Carolina Carrere, Acevedo Rubén, and Tabernig Carolina*

Hybrid Brain-Computer Interface for Attention Training in Adolescents with Attention Deficit: A Proof-of-Concept Study . . . . . . . . . . 500
*M. Belén Masset, Carolina B. Tabernig, and L. Carolina Carrere*

FMRI Paradigm to Neurorehabilitation: Preliminary Experimentation . . . . . . . . . . 509
*Daniela Pedrozo, Juan Pablo Graffigna, Elisa Perez, Emanuel Tello, Alejandro Rodrigo, Cecilia Rollan, and Daniela Bazán*

Postural Stability in Virtual Reality Environments: Analysis of Different Conditions of the Afferent Systems . . . . . . . . . . 521
*Fernando Tettamanti, Juan Iturrieta, Alejandro Yanadel, Natalia Lópes, and Elisa Pérez*

Serious Game Design for Elderly People Based on Their Interests and Motivations . . . . . . . . . . 533
*Juan C. Iturrieta, Alejandro R. Yanadel, Vicente Mut, Natalia M. López, and M. Elisa Perez*

Identification of Motor Patterns in Functional Activities Related to ADLs . . . . . . 551
*Emanuel B. Tello, Alejandro R. Yanadel, M. Elisa Perez, and Natalia M. López*

**Author Index** . . . . . . . . . . 567

# Biomedical Signal Processing

# Improved ERD Detection of EEG Sensorimotor Rhythms Through Wavelet Transform

Alejandro Quiroga[1(✉)], Diana Vértiz del Valle[1], Katherine Tschopp[1], Leonardo Rufiner[2,3], and Rubén Acevedo[1]

[1] Center of Rehabilitation Engineering and Neuromuscular Research, Faculty of Engineering, National University of Entre Ríos, Oro Verde, Entre Ríos, Argentina
alejandro.quiroga@uner.edu.ar

[2] Institute for Signals, Systems and Computational Intelligence, sinc(i), UNL-CONICET, Ciudad Universitaria UNL, 4th Floor, FICH, Santa Fe, Argentina

[3] Cybernetics Laboratory, Faculty of Engineering, National University of Entre Ríos, Concepción del Uruguay, Entre Ríos, Argentina

**Abstract.** Brain-computer interfaces are a novel tool to implement neurorehabilitation therapies in people with motor disabilities. One of the most used paradigms in neurorehabilitation is the one based on the electroencephalogram. During the execution or attempted execution of a movement, a decrease in sensorimotor rhythms occurs in the contralateral hemisphere known as event-related desynchronization (ERD). Power spectral density is widely used in the literature to detect ERD, under the assumption that SMRs are rhythmically sustained oscillations. A recent theory suggests that neural oscillations can be represented as rhythmically sustained oscillations with dynamic amplitude or also as bursts without underlying rhythmicity. This allows the use of the wavelet transform, in particular the discrete dyadic wavelet transform (DDWT), which has a representation through compact support functions that allows highlighting localized frequency characteristics of a signal. In this work, the performance of different DDWT-based feature extraction strategies and denoising techniques were compared in order to improve the performance of ERD detection of SMR. The DDWT with the bior2.8 wavelet and a polynomial SVM classifier yielded the best performance, achieving a high true positive rate. However, the overall accuracy did not match the favorable results. To address this limitation, future research incorporating data augmentation techniques and feature selection algorithms are proposed to reduce the dimensionality of the data.

**Keywords:** Wavelet transform · DDWT · BCI · ERD

## 1 Introduction

Brain Computer Interfaces (BCI) are a novel tool to implement neurorehabilitation therapies in people with motor disabilities. By decoding brain activity, BCIs can interpret user intentions and generate corresponding outputs [1]. One of the most used paradigms in neurorehabilitation is the one based on electroencephalogram (EEG), whose recording


F. E. Ballina et al. (Eds.): SABI 2023, IFMBE Proceedings 114, pp. 3–13, 2024.
https://doi.org/10.1007/978-3-031-61973-1_1

is done in the central area located on the sensorimotor cerebral cortex. During the execution or attempted execution of a movement, there is a decrease in sensorimotor rhythms (SMR) in the contralateral hemisphere known as event related desynchronization (ERD).

Power Spectral Density (PSD) is widely used in the literature for detecting ERD of SMRs [2], this assumes that the SMRs are rhythmically sustained oscillations. However, a recent theory has emerged suggesting that neural oscillations, which include SMRs, can also be represented as rhythmically sustained oscillation with amplitude dynamics and as burst-events with no underlying rhythmicity, see Fig. 1. The “bursting” interpretation comes with far-reaching implications, but its importance depends on its being an accurate reflection of physiology measures [3].

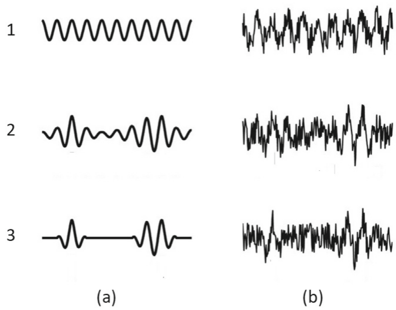


**Fig. 1.** Types of neural oscillations: (1) Rhythmically sustained oscillation without amplitude dynamics, (2) Rhythmically sustained oscillation with amplitude dynamics, (3) Burst-events with no underlying rhythmicity. (a) without noise and (b) with noise. Adapted from [3].

This makes us suppose that a representation of the signal using elements of short duration, and with a defined temporal location, would allow a better representation of the signal. Wavelet representation has a compact support that allows highlighting localized characteristics of a signal, such as those shown in Fig. 1 (2.a) and (3.a) in the time-frequency plane. This uses windows of different sizes, so that high frequencies are evaluated in the shorter window and low frequencies in the longer window. Therefore, it provides a flexible framework, from which it is possible to compactly represent different characteristics of the signal. [4]. In particular, the discrete dyadic wavelet transform (DDWT) is one of the most commonly used methods to generate orthogonal bases from the wavelet transform, due to its simple and inexpensive computational implementation.

The aim of this work was to analyze and compare extracting features strategies based on DDWT, using different wavelet mother functions and denoising techniques, in order to improve the performance of ERD detection of SMRs.

## 2 Methods

### 2.1 EEG Dataset

The dataset used in this work was obtained from the Center for Neuromuscular and Sensory Rehabilitation and Research Engineering (CIRINS) at the Faculty of Engineering of the National University of Entre Ríos. The dataset comprised EEG signals from six volunteers without neurological or cognitive sequelae. The signals were recorded using the IM-tention software with a sampling frequency of 250 Hz and five recording channels in a monopolar configuration [5]. The electrodes were located at C3, Pz, C4, Fz and Cz; the ground and reference electrodes were placed at A1 and A2 respectively. For EEG signals preprocessing, a 2nd order bandpass Butterworth filter (1–40 Hz) and a notch filter to reject power line frequency of 50 Hz were used. To emphasize localized activity on the Cz electrode, a Laplacian spatial filter was used [1] (Fig. 2).

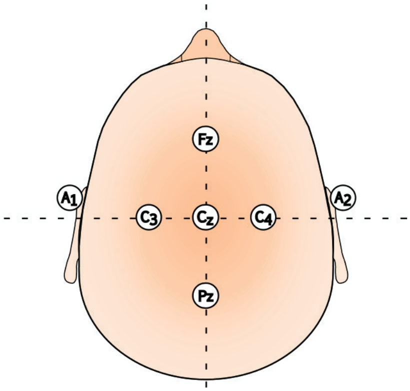


**Fig. 2.** Electrodes used in the EEG dataset.

Considering the stages needed in order to use a BCI, records were obtained in the calibration stage (calibration recordings) and in the closed-loop stage (online recordings). In the calibration recordings, visual cues (arrows presented on a monitor) were used to indicate which foot the volunteer should move (right or left) as well as when it should be at rest (pause sign). These visual instructions were randomly repeated 10 times for each foot during each series of recordings. Three series of EEG recordings were conducted for each volunteer. Then, temporal patterns were formed by segmenting the EEG signals using temporal marks that identified the appearance time of the visual cue. This process defined intervals corresponding to movement and rest, as illustrated in Fig. 3. The 500 ms following the visual cue were discarded, and the subsequent 2 s were considered as the interval during which the subject performed the movement. Similarly, the 500 ms preceding the cue were discarded and the 2 s prior were considered as the rest interval.

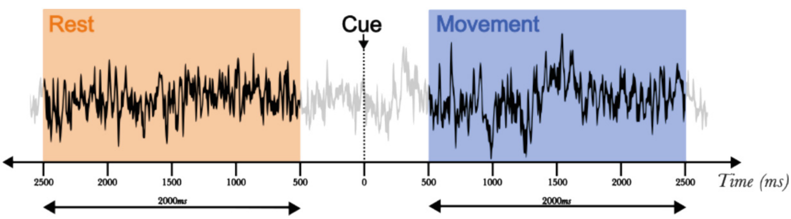


**Fig. 3.** EEG signal segmentation.

In the case of online recordings, three series were conducted, each consisting of 10 movements of the dominant foot and 10 rest periods. It is important to note that only actual foot movements were performed, with no attempted movements, in order to ensure the manifestation of the ERD, as the objective of this work is to evaluate the ERD detection.

### 2.2 Features Extraction Strategies

This section describes the feature extraction strategies evaluated in this work.

#### 2.2.1 Power Spectral Density

Since ERD is a power decrease of SMR, the power spectral density (PSD) of temporal patterns was computed. There are different approaches to estimate the PSD and in this work, Welch's method for PSD estimation was employed. This approach divides the signal into overlapping windows, estimates the periodogram for each window, and averages them to obtain the PSD [6].

In the calibration stage, the PSD of the temporal patterns was calculated using the Welch method with 1Hz resolution and 3 Hamming windows of 1 s (50% overlapping). This process resulted in two sets of 23 features (referred to as feature vectors), including only the frequencies in the 8–30 Hz range which correspond to SMR. During the Closed-loop stage, a single feature vector is extracted only from the movement interval.

#### 2.2.2 Dyadic Discrete Wavelet Transform

The wavelet transform is an important tool for signal processing, as it allows the representation of signals in the time-frequency plane and provides detailed analysis at both high and low frequencies (multiresolution analysis) as well as good response when dealing with nonstationary signals [7]. The wavelet transform is achieved by calculating the inner product between the signal of interest and the wavelet function ($\phi$) at a scale and translation, determined by the scale function ($\psi$). This process yields coefficients corresponding to an orthogonal base which represents the original signal into different resolution levels.

In this work, the dyadic discrete wavelet transform (DDWT) was used, with a scaling factor of 2, resulting in a more efficient transform compared to the continuous-time wavelet transform. This is because the DDWT produces fewer coefficients and reduces redundant information. The state of the art analysis brings a number of wavelet functions used in common EEG feature extraction problems [8]. Considering the similarity between the morphology of the wavelet functions and the bursts mentioned earlier, the following families of wavelet functions were chosen: Daubechies (db4, db6, db10, db13, db14 and db15), Biorthogonal (bior2.4, bior2.8, bior3.1, bior5.5 and bior6.8), Coiflet (coif5) and Symlet (sym5). Figure 4 shows an example for each of the selected families.

The DDWT algorithm implementation involves a tree decomposition (see Fig. 5) using a filter bank approach. At each decomposition level, a low-pass filter and a high-pass filter are applied to extract a set of coefficients known as approximation (A) and detail (D), respectively. Dyadic scaling allows to reduce the number of the coefficients

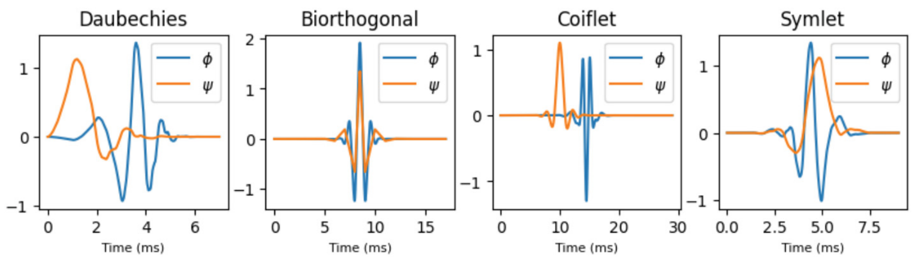


**Fig. 4.** Examples of Daubechies, Biorthogonal, Coiflet and Symlet wavelet families.

of the previous level by half and enables the representation of specific frequencies using any selected coefficients.

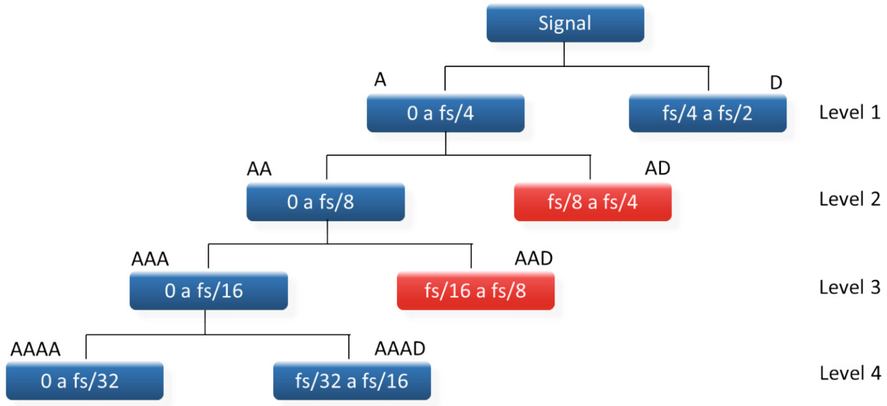


**Fig. 5.** DDWT tree decomposition.

As previously mentioned, the sample frequency was fs = 250 Hz, resulting in a maximum signal frequency of 125 Hz. Based on this, at level 1, the decomposition consists of A and D, representing frequencies from 0 Hz to 62.5 Hz and 62.5 Hz to 125 Hz respectively. The level 2 consists of AA and AD, representing frequencies from 0 Hz to 31.25 Hz and AD 31.25 Hz to 62.5 Hz respectively. Continuing this pattern, AAA and AAD represent frequencies from 0 Hz to 15.625 Hz and 15.625 Hz to 31.25 Hz respectively at level 3. Finally, on level 4 AAAA represents frequencies from 0 Hz to 7.81 Hz and AAAD represents frequencies from 7.81 Hz to 15.625 Hz.

To focus on the frequency range of interest for SMRs (8–30 Hz), a denoising scheme was applied. Only the coefficients corresponding to AAAD and AAD (7.81 Hz to 31.2 Hz) were used. These coefficients are then concatenated to form the feature patterns, as shown in blue in Fig. 5.

### 2.3 Classifiers

According to [9], Fisher's linear discriminant analysis (LDA) and support vector machine (SVM) are suitable classifiers for studying the ERD phenomenon. Therefore, in this work, both LDA and SVM classifiers were implemented and compared.

#### 2.3.1 Linear Discriminant Analysis

Fisher's linear discriminant is a linear classifier with easy implementation and low computational cost. It assumes that the classes are normally distributed with identical covariance (homoscedasticity assumption). Though the LDA classifier imposes very strong assumptions on the distribution of the data, the computation of the discriminative function is very efficient, that's why it has been popular in the BCI field [10].

The LDA, like any binary linear classifier, can be characterized by the Eq. (1):

$$\mathrm{g(z)} = \mathrm{w}^{\mathrm{T}} \cdot \mathrm{z} + b \tag{1}$$

where $w = [w_1 \ldots w_k]$ is the projection vector, $z \in R^k$ represents the input vector and $b$ is the bias term. The classification function assigns the class label $\mathrm{C_i}$ to each pattern z depending on the sign of the function g(z). It is assumed that the probability distributions of each class follow a Gaussian distribution.

#### 2.3.2 Support Vector Machine

One of the widely used classifiers in BCI for various applications is the Support Vector Machine (SVM), a kernel-based classifier [11]. For the specific problem addressed in this work, which involves 2 classes, SVM finds a hyperplane that separates the classes. This process involves projecting the data into a high-dimensional space, where the classes could be linearly separable. In cases where linear separability cannot be achieved, the use of appropriate kernel functions becomes necessary. Although different kernel functions were evaluated, this work presents the results obtained using the linear and polynomial kernels (Eq. 2), as they demonstrated the highest performance.

$$(<x, y> + c)^d, c \in \Re, d \in \aleph \tag{2}$$

In the SVM training process, grid-search and cross-validation techniques were employed to optimize the classifier's performance. Grid-search involved varying the values of key parameters, such as C, gamma ($\gamma$), and the polynomial degree. For the linear kernel, the parameter C determines the trade-off between misclassification and maximizing the margin. In the case of the polynomial kernel, $\gamma$ controls the influence of individual training samples and the polynomial degree sets the degree of the polynomial kernel function.

Cross-validation was used to evaluate the performance of the SVM with a linear kernel across different C values and the SVM with a polynomial kernel using different parameter combinations. The selection of the optimal parameter set was based on the accuracy metric. In this work, the chosen parameters ranges were as follows: C values ranged from $10^{-2}$ to $10^{10}$, $\gamma$ values ranged from $10^{-9}$ to $10^{3}$ and the polynomial degree values were set to 2 and 3. These ranges were selected based on prior knowledge [12] and experimentation. Using grid-search and evaluating performance through cross-validation, the SVM classifier was fine-tuned to achieve the highest accuracy result.

### 2.4 Performance Metrics

In the calibration stage, the performance of the classifier was evaluated using the Accuracy ($Acc_{Cal}$) metric, the feature vectors obtained in this stage were used. The objective of this metric is to estimate the effectiveness of the calibration process. In the closed-loop stage, the Accuracy (*Acc)* and True Positives Rate (*TPR*) were employed. These metrics can be calculated using the Eqs. (3) and (4), where *TP* represents true positives, *TN* represents true negatives, *FP* represents false positives, and *FN* represents false negatives.

$$Acc\,[\%] = \frac{TP + TN}{TP + TN + FP + FN}.100 \tag{3}$$

$$TPR\,[\%] = \frac{TP}{TP + FN}.100 \tag{4}$$

In the context of neurorehabilitation, reporting the TPR is crucial because the BCI is active only during the execution or attempted execution of a movement. The rest of the time, the BCI remains inactive, which means that only the class related to the movement is available.

## 3 Results

To select the best wavelet functions within each family, the *TPR* at the close-loop was used instead of *Acc* due to the minimal variability between wavelet functions. Therefore, the *TPR* was analyzed using the three classifiers: LDA, SVM with linear kernel and SVM with polynomial kernel. In the case of the Daubechies family, the db6 wavelet function achieved the highest rate, as can be seen in Table 1; for the Biorthogonal family, the bior2.8 function demonstrated the highest rate, as shown in Table 2. This selection was not necessary for Coiflet and Symlet families, since only one function per family was considered.

**Table 1.** Daubechies family TRP results

| *Wavelet function* | *Median TPR* | | |
|---|---|---|---|
| | LDA | kernel = Linear | kernel = Poly |
| *db4* | 50.00 | 50.50 | 61.11 |
| ***db6*** | **63.33** | **55.00** | **85.00** |
| *db10* | 55.00 | 51.11 | 57.77 |
| *db13* | 60.55 | 54.17 | 50.00 |
| *db14* | 55.55 | 49.16 | 66.11 |
| *db15* | 55.55 | 50.00 | 65.55 |

**Table 2.** Biorthogonal family TRP results

| *Wavelet function* | *Median TPR* | | |
|---|---|---|---|
| | LDA | kernel = Linear | kernel = Poly |
| *bior2.4* | 61.66 | 50.55 | 91.11 |
| ***bior2.8*** | **66.70** | **58.30** | **96.70** |
| *bior3.1* | 53.00 | 57.78 | 92.22 |
| *bior5.5* | 57.22 | 53.33 | 75.55 |
| *bior6.8* | 56.66 | 56.67 | 79.45 |

The Fig. 6, 7 and 8 shows the results comparison between the best wavelets functions and the PSD, using the latter as a reference.

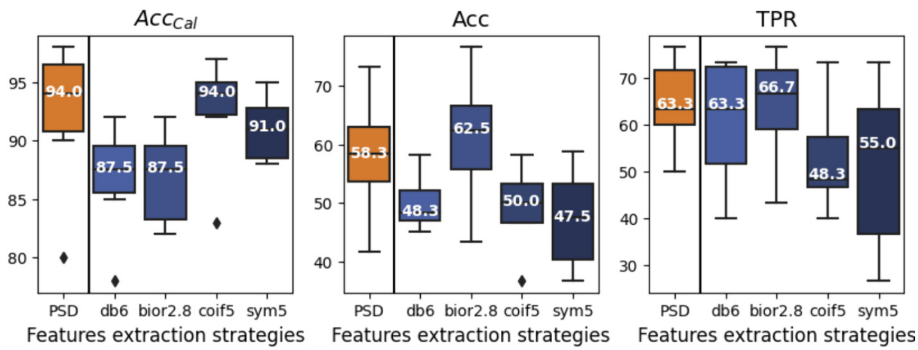


**Fig. 6.** Performance metrics using LDA.

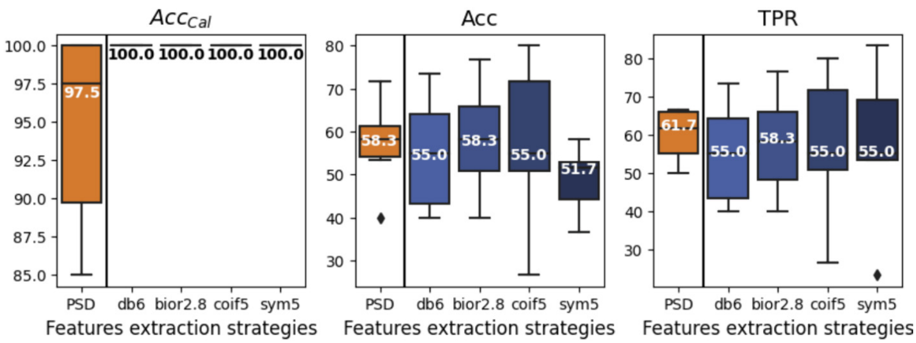


**Fig. 7.** Performance metrics using linear SVM.

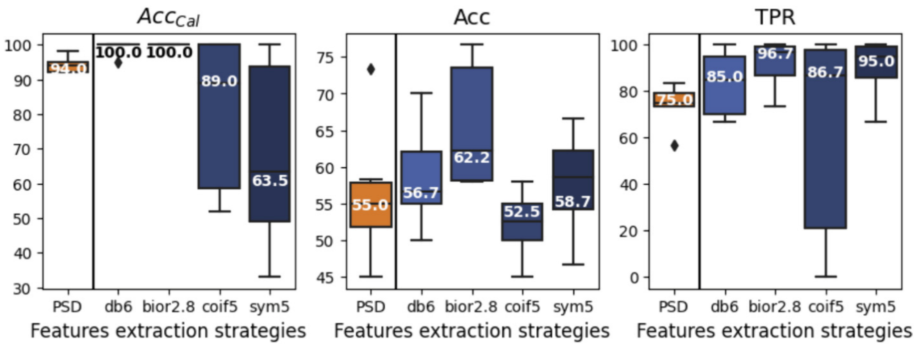


**Fig. 8.** Performance metrics using SVM with polynomial kernel.

By analyzing the previous figures, it was found that higher *TPR* is obtained by using bior2.8 wavelet function, the best case being the use in combination with the SVM with polynomial kernel. Figure 9 shows a comparison with the reference (PSD).

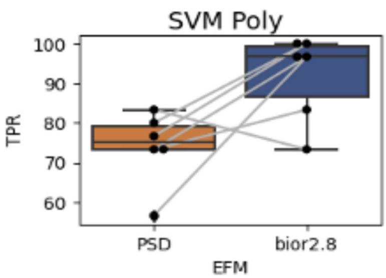


**Fig. 9.** Statistical analysis for PSD and bior2.8

A repeated measures ANOVA test (Anova-RM) was used to assess differences in TPR between bior2.8-SVM polynomial and the PSD-LDA combinations, the results are shown in Table 3.

**Table 3.** Anova-RM analysis for PSD and bior2.8

| | F Value | Num DF | Den DF | Pr > F |
|---|---|---|---|---|
| Features extraction strategies | 6.8088 | 1.0000 | 5.0000 | 0.0477 |

## 4 Conclusions

This paper presented a comparison of feature extraction strategies based of DDWT to detect ERD of sensorimotor rhythms for potential use in a BCI for neurorehabilitation.

According to the results obtained, the combination of bior2.8 wavelet function and SVM polynomial outperformed the other alternatives in terms of the *TPR* (96,7%). Statistical analysis revealed a significant difference between bior2.8-SVM polynomial and the PSD-LDA combination, as indicated by a p-value below 0.05. However, it is important to keep in mind that *TPR* cannot be the only metric to draw a definitive conclusion, as high *TPR* may bias the results. This is clear, since the *Acc* for this combination is 62.2%, this implies that in this case the classifier has high sensitivity and low specificity. Future work should aim to improve the performance of the classifier trying to increase the *Acc* and consequently the specificity.

On the other hand, using wavelet functions as a feature extraction strategy can improve classification metrics due to the relationship between the burst events theory and the morphology of wavelet functions. This is evidenced through their inner product, as demonstrated by the similarity between the signal in Fig. 1 (2.a) and (3.a) and the wavelets functions in Fig. 4.

Another aspect to consider when analyzing the results is the limited amount of data available to train the classifiers (30 samples per class). This may have contributed to the challenges in achieving a good generalization by the strategies presented in this paper. To address this limitation in future works, it is proposed to employ data augmentation techniques as well as feature selection algorithms to reduce the dimensionality of the data.

**Acknowledgments.** This work was funded by the PID-UNER #6235 *"Application of machine learning to biomedical problems in the context of sparse data"* and CAID-UNL 50620190100151LI *"Algoritmos inteligentes profundos para análisis y clasificación de bioseñales"*.

## References

1. Wolpaw, J.R., Wolpaw, E.W. (eds.): Brain-Computer Interfaces: Principles and Practice. Oxford University Press, 400 p. Oxford, New York (2012)

2. Lotte, F., Bougrain, L., Cichocki, A., Clerc, M., Congedo, M., Rakotomamonjy, A., et al.: A review of classification algorithms for EEG-based brain–computer interfaces: a 10 year update. J. Neural Eng. **15**(3), 031005 (2018)
3. van Ede, F., Quinn, A.J., Woolrich, M.W., Nobre, A.C.: Neural oscillations: sustained rhythms or transient burst-events? Trends Neurosci. **41**(7), 415–417 (2018)
4. Acevedo, R., Atum, Y., Gareis, I., Biurrun Manresa, J., Medina Bañuelos, V., Rufiner, L.: A comparison of feature extraction strategies using wavelet dictionaries and feature selection methods for single trial P300-based BCI. Med. Biol. Eng. Comput. **57**(3), 589–600 (2019)
5. del Valle, D.V., Carrere, C., Acevedo, R., Tabernig, C.: IM-tention: a software for brain computer interfaces with motor recovery purposes. In: SABI 2023, IFMBE Proceedings 114, vol. II, pp. 1–11 (2024). https://doi.org/10.1007/978-3-031-61973-1_46
6. Gursel Ozmen, N., Gumusel, L., Yang, Y.: A biologically inspired approach to frequency domain feature extraction for EEG classification. Comput. Math. Methods Med. **23**(2018), e9890132 (2018)
7. Rufiner, H.L., Goddard, C.J.: A method of wavelet selection in phoneme recognition. In: Proceedings of 40th Midwest Symposium on Circuits and Systems Dedicated to the Memory of Professor Mac Van Valkenburg, vol. 2, pp. 889–891 (1997)
8. Ganorkar, S., Raut, V.: Comparative analysis of mother wavelet selection for EEG signal application to motor imagery based brain-computer interface. **8**(12) (2019)
9. Quiroga, A., del Valle, D.V., Pilz, M., Acevedo, R.: Performance comparison of different classifiers to detect motor intention in EEG-based BCI. In: Marques, J.L.B., Rodrigues, C.R., Suzuki, D.O.H., Marino Neto, J., García Ojeda, R. (eds.) CLAIB CBEB 2022. IFMBE Proceedings, vol. 100, pp. 90–101. Springer, Cham (2024). https://doi.org/10.1007/978-3-031-49407-9_10
10. Bashashati, H., Ward, R.K., Birch, G.E., Bashashati, A.: Comparing different classifiers in sensory motor brain computer interfaces. PLoS ONE **10**(6), e0129435 (2015)
11. Rasheed, S.: A review of the role of machine learning techniques towards brain-computer interface applications. Mach. Learn. Knowl. Extr. **3**(4), 835–862 (2021)
12. Quitadamo, L.R., et al.: Support vector machines to detect physiological patterns for EEG and EMG-based human-computer interaction: a review. J. Neural Eng. **14**(1), 011001 (2017)

# Optimized Transcranial Brain Stimulation for Tumor Treating Fields

Dante C. Andrinolo O.[1(✉)], Mariano Fernández-Corazza[1], and Carlos H. Muravchik[1,2]

[1] LEICI Instituto de Investigaciones en Electrónica, Control y Procesamiento de Señales (UNLP-CONICET), Buenos Aires, Argentina
dante.andrinolo@alu.ing.unlp.edu.ar, {marianof.corazza,carlosm}@ing.unlp.edu.ar

[2] Comisión de Investigaciones Científicas, CICPBA, Buenos Aires, Provincia de Buenos Aires, Argentina

**Abstract.** Transcranial electrical stimulation (TES) is a field that investigates the effects of applying low-intensity electrical currents to the human brain using electrodes placed on the scalp. Tumor Treating Fields (TTFields) is one application of TES, that consists of applying alternating electric fields ($\sim$300 KHz) to a tumoral region to arrest its growth. The physiological principle is that tumoral cells are killed during the mitosis if the fields are aligned with the cell subdivision direction. The conventional protocol involves switching between two ad-hoc and intuitive anterior-posterior and left-right stimulation patterns. This paper focuses on optimizing the current injection patterns to stimulate the tumoral region, maximizing the average electric field intensity inside the tumor along predefined electric field orientations. The reciprocity theorem is used to optimize the current injection using two electrode arrays: the conventional 36-electrode TTFields array and the 64-electrode 10–20 electroencephalography array. A realistic head model, including brain tissues and a tumor, is used to solve the forward problem of TES using the finite element method. The performance is evaluated based on the directionality and intensity metrics of the electric field within the tumor. The results show improved performance in terms of directionality and intensity for the optimized patterns compared to the conventional protocol. The proposed optimization approach has the potential to enhance the efficacy of TTFields.

**Keywords:** TTFields · Transcranial Electrical Stimulation (TES) · Optimal Electrical Stimulation · Reciprocity Theorem

## 1 Introduction

Transcranial electrical stimulation (TES) is a rapidly evolving field in bioengineering and neuroscience that explores the effects of applying minimally-invasive 'low' intensity electrical currents to the human brain. TES relies on applying an


F. E. Ballina et al. (Eds.): SABI 2023, IFMBE Proceedings 114, pp. 14–21, 2024.
https://doi.org/10.1007/978-3-031-61973-1_2

electrical current through two or more electrodes (array of electrodes) placed on the scalp to modify or modulate cortical excitability and brain function. Alternate and direct current TES are known as tACS and tDCS respectively. Research has demonstrated that TES can be a valuable therapeutic tool for the treatment of epilepsy, Parkinson's disease, anxiety, and stroke rehabilitation [1]. They also proposed to enhance cognitive skills such as memory or learning [1]. In this work we focus on the application of TES for treating tumors.

In TES, the current injected by each electrode of the array, known as current injection pattern, produces an electric field (or current density) map on the brain [2,3]. The computation of this map is known as the forward problem (FP), typically solved numerically using the finite element method (FEM) in a realistic human head model [4]. The electrical conductivity and the shape of the different head tissues determine the spatial distribution of the electric fields [3]. The inverse problem (IP) is to determine the current injection pattern that stimulates a certain region of interest (ROI) in a desired way. Depending on the criteria, several optimization schemes have been proposed leading to different solutions.

Tumor treating fields (TTFields) therapy is a case of tACS applied to the treatment of glioblastoma multiforme (GBM). It consists in delivering intermediate-frequency electric fields to the tumoral region, arresting the growth of cancerous cells due the interference with mitosis and cytokinesis [2]. If an electric field of $\sim$100–300 KHz of frequency and 0.5–3 V/cm of intensity is applied to a GBM, the cellular growth can be disrupted [5,6]. The electric field aligned to the cell-division preferred orientation is believed to affect metaphase by disrupting mitotic spindle formation, and anaphase, by dielectrophoretic dislocation of intracellular constituents, resulting in apoptosis [2]. Because the healthy cells of the brain do not divide frequently in comparison to the GBM cells, TTFields leaves the healthy cells relatively unaffected [6]. It was experimentally found in vitro that the technique is more efficient if more directions are covered [7].

The conventional protocol for TTFields use 4 arrays of 9 capacitive electrodes each, positioned on the right, left, anterior and posterior regions of the scalp (called here *TTFields array*) [5]. The injected current for this method is 100mA per electrode with a total current of 900mA. The injection pattern switches, between left to right (LR) and anterior to posterior (AP), expecting to generate electric fields inside the tumor along two orthogonal directions of the 3D space.

However, the conventional protocol relies on pure intuition and hence, is not optimal. LR or AP stimulation on the scalp does not guarantee the largest, most orthogonal or most directional electric fields within the tumor. To improve the orthogonality and intensity of the fields, the current injection patterns require optimization.

This work uses the reciprocity theorem optimization methodology to maximize the electric field intensity inside the tumor along the three canonical orientations (LR, AP and bottom-up or BU), with the TTFields array (36 electrodes) and with the standard 10–20 electroencephalography (EEG) 64-electrode system (considering 18 active electrodes in all cases).

## 2 Methods

### 2.1 Head Model

We used a realistic head model based on the ICBM-152 atlas with five tissues: brain (BR), cerebrospinal fluid (CSF), skull (SK), scalp (SC), and the tumor. We extracted, meshed and generated the 3D surfaces, to produce a tetrahedral volumetric mesh from these surfaces, with the Iso2mesh library. The final tetrahedral mesh has around of 950.000 elements and 160.000 nodes ($N$). The proposed tumor was modeled as a sphere of 0.5 cm radius, placed at 1.8cm under the central sulcus, biased 1.2 cm towards the right hemisphere. Each tissue was assumed to be homogeneous and isotropic conductivity with values 0.25, 1.79, 0.01, 0.25 and 0.24 S/m assigned to BR, CSF, SK, SC and tumor respectively [2]. The model considers two pointwise electrode arrays, the TTFields $4 \times 9$ electrode array [5], and the standard 10–20 EEG 64 electrode array, shown in Fig. 1. We manually determined the TTFields array electrode locations based on anatomical landmarks and visual inspection. The 10–20 standard array was projected to the scalp surface from the standard spherical coordinates.

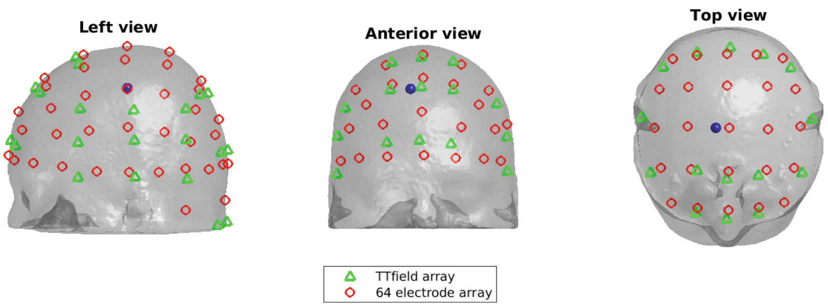


**Fig. 1.** Plot of the scalp surface and the tumor (in blue). TTFields electrodes and 10–20 EEG 64 electrodes are plotted as green triangles and red circles respectively.

### 2.2 TES Forward Problem

The solution of the FP requires solving the electromagnetic physical (Maxwell's) equations. Given the frequency range of the problem, the quasi-static approximation is applicable [8,9]. Assuming a pointwise electrode model, the mathematical formulation is established as:

$$\begin{cases} \vec{\nabla} \cdot (\boldsymbol{\sigma}(\vec{x})\vec{\nabla}\Phi(\vec{x})) = 0, & \text{in } \Omega \\ \boldsymbol{\sigma}(\vec{x})(\vec{\nabla}\Phi(\vec{x})) \cdot \hat{n} = j(\vec{x}), & \text{in } \delta\Omega \end{cases} \tag{1}$$

where $\Omega$ is the head solid, $\delta\Omega$ is its boundary, $\vec{x}$ is an arbitrary location in space, $\Phi$ is the electric potential, $\boldsymbol{\sigma}$ is the tensor conductivity, $j$ is the normal component of the current density on the external surface, and $\hat{n}$ is the normal to the boundary vector.

This equation system is solved using the first order FEM with the Galerkin approach, that converts the FP (1) into a linear system of equations $\boldsymbol{Kv} = \boldsymbol{f}$, where $\boldsymbol{K}$ is the $N \times N$ *stiffness* matrix computed using the geometry and conductivity map of each tissue, $\boldsymbol{v}$ is the $N \times 1$ unknown vector of electric potential and $\boldsymbol{f}$ is the $N \times 1$ vector of injected current [3,10]. An arbitrary electrode is used as a reference for the electric potential and thus, the range of $\boldsymbol{K}$ is $N-1$ implying that $K$ is not an invertible matrix. The algorithm used to solve this linear system is the preconditioned conjugated gradient algorithm with the LU factorization as preconditioner [11]. After $\boldsymbol{v}$ is determined, the numerical gradient operator is calculated in order to get the electric field at the ROI.

Due to the linear nature of the electric fields, any current injection pattern can be obtained as a linear combination of a complete set of independent elementary patterns. Then, if there are $L$ electrodes, $L-1$ independent injection patterns are needed to form a complete set. Each independent pattern was modeled as an $L$-dimensional vector $p_i$, with $I_{max}$ at the $i$-th electrode and $-I_{max}$ at the reference electrode, where $I_{max}$ is the maximum current allowed per electrode.

Then, the electric field was computed for all ROI tetrahedrons and for each elementary current injection pattern leading to a $3T \times (L-1)$ dimension matrix $\boldsymbol{T_M}$ known as *transfer matrix* ($T$ is the number of ROI tetrahedrons). The resulting electric field for an arbitrary current injection pattern $\boldsymbol{c}$ is obtained as $\boldsymbol{E} = \boldsymbol{T_M}\,\boldsymbol{c}$.

### 2.3 Inverse Problem

We solved the IP applying the reciprocity theorem for TES and EEG, that maximizes the average electric field intensity at the ROI along a predefined direction [3].

**Reciprocity Theorem as an Optimization Method.** The reciprocity theorem coupling between TES and EEG is formulated as:

$$\boldsymbol{\Phi}(a) - \boldsymbol{\Phi}(b) = \frac{\vec{d} \cdot \vec{\nabla}\boldsymbol{\psi}_{ab}(\vec{x})}{I_{ab}} \tag{2}$$

where $\boldsymbol{\Phi}(p)$ is the electric potential at an arbitrary point of the boundary $p$ produced by a dipolar electrical source $\vec{d}$ in $\vec{x}$, and $\vec{\nabla}\boldsymbol{\psi}_{ab}(\vec{x})$ is the gradient of the impressed potential (or minus the electric field) at $\vec{x}$ when a current is injected between locations $a$ and $b$. Assuming that $\vec{d}$ is the desired direction for the impressed electric field, to maximize the dot product of $\vec{d}$ and the electric field at $\vec{x}$, $\boldsymbol{\Phi}(a) - \boldsymbol{\Phi}(b)$ should be maximized, therefore, $a = A$ and $b = B$